

**PROBING THE QCD VACUUM  
WITH FLAVOUR SINGLET OBJECTS:  
 $\eta'$  ON THE LATTICE**

T. STRUCKMANN<sup>a</sup>, K. SCHILLING<sup>a,b</sup>, P. ÜBERHOLZ<sup>b</sup>  
N. EICKER<sup>b</sup>, S. GÜSKEN<sup>b</sup>, TH. LIPPERT<sup>b</sup>, H. NEFF<sup>a</sup>, B. ORTH<sup>b</sup>,  
J. VIEHOFF<sup>a</sup>,

<sup>a</sup>*NIC, Forschungszentrum Jülich, 52425 Jülich and  
DESY, 22603 Hamburg, Germany  
k.schilling@fz-juelich.de*

<sup>b</sup>*Fachbereich Physik, Bergische Universität, Gesamthochschule Wuppertal  
Gaußstraße 20, 42097 Wuppertal, Germany*

(SESAM - T $\chi$ L Collaboration)

We present a study on the direct determination of the  $\eta'$  mass on the full set of SESAM and T $\chi$ L QCD vacuum configurations with 2 active flavours of Wilson fermions, at  $\beta = 5.6$ . We observe a definite dependency of the two-loop correlator on the topological charge sector.

## 1 Introduction

Flavour symmetric hadronic states are of particular importance for the understanding of nonperturbative aspects of quantum chromodynamics (QCD). In fact they are expected to reveal important insight into the topological vacuum structure induced by gluonic self interactions, as borne out in the famous Witten-Veneziano formula<sup>1</sup> that relates the flavour octet/singlet mass splitting,  $M_0^2$ <sup>a</sup>, to the topological susceptibility,  $\chi_q$ , in the large- $N_c$  limit of the theory:

$$M_0^2 := M_{\eta'}^2 - M_8^2 = 2N_f \chi_q / f_\pi^2, \quad (1)$$

with  $N_f$  being the number of active flavours and  $f_\pi$  the pion decay constant.

While glueballs have been the target of many *ab initio* lattice investigations over the past fifteen years<sup>2</sup> much less attention has been paid to the direct calculation of flavour singlet states *with fermionic content* such as the  $\eta'$  meson. The reason is obvious: the extraction of flavour singlet mesons from

<sup>a</sup>Upper (lower) case letters refer to masses in physical (lattice) units.

Table 1: Lattice parameters and numbers of independent vacuum field configurations and stochastic sources,  $N_e^U$ . Last two columns: t-ranges for the single exponential fits to the octet and singlet channel correlators.

$\kappa_{sea}$	$m_\pi/m_\rho$	$L^3 * T$	$N_e^U$	$N_{conf}$	$G_8$ -Fit	$G_{\eta'}$ -Fit
0.1560	0.834(3)	$16^3 * 32$	400	195	12 – 16	6 – 9
0.1565	0.813(9)	$16^3 * 32$	400	195	13 – 16	6 – 9
0.1570	0.763(6)	$16^3 * 32$	400	195	12 – 15	6 – 9
0.1575	0.692(10)	$16^3 * 32$	400	195	12 – 15	6 – 9
0.1575	0.704(5)	$24^3 * 40$	400	156	12 – 15	6 – 9
0.1580	0.574(13)	$24^3 * 40$	100	156	12 – 15	6 – 9

the lattice is even more challenging than the one of glueball states, due to the substantial cost of computing quark (rather than Wilson) loop correlators. In fact such Zweig-rule forbidden diagrams (in general misleadingly called ‘disconnected diagrams’) consist of two quark loops connected via gluon lines only and need to be calculated in the momentum zero state, which amounts to the computationally very expensive evaluation of the trace of the inverse Dirac operator. The two pioneering studies in the field used quenched vacuum configurations, with Wilson fermions and wall sources<sup>3</sup> and staggered fermions with stochastic sources<sup>4</sup>.

This situation will change with the imminent advent of near-Teraflops computers that promise both to provide (a) sufficient sampling rates for full QCD vacuum configurations and (b) the analysing power to deal with the above mentioned loop-loop correlators. Albeit present day simulations are still restricted to the case of two active flavours,  $N_f = 2$ , it is of great interest to fathom state-of-the art techniques to deal with Zweig rule forbidden diagrams. First results on flavour singlet masses were presented recently by CP-PACS<sup>5</sup> and UKQCD<sup>6</sup>.

In the present paper we present a study on the  $\eta'$  mass using the full set of QCD configurations generated by SESAM ( $16^3 \times 32$ , ‘small lattice’) and T $\chi$ L<sup>7</sup> ( $24^3 \times 40$ , ‘large lattice’), both at  $\beta = 5.6$  with standard Wilson action (see Table 1).

## 2 Disconnected diagrams

## 2.1 The problem

We consider the pseudoscalar flavour singlet operator in a flavour symmetric theory

$$\eta'(x) = \sum_{i=1}^{N_f} \bar{q}_i(x) \gamma_5 q_i(x) , \quad (2)$$

with  $N_f$  flavours. By the usual Wick contraction it leads to the flavour singlet propagator in terms of the inverse Dirac operator,  $M^{-1}$ :

$$\begin{aligned} C_{\eta'}(0|x) &\sim N_f \text{tr}((M^{-1}(0|x))^\dagger M^{-1}(0|x)) \\ &\quad - N_f^2 \text{tr}(\gamma_5 M^{-1}(0|0))^\dagger \text{tr}(\gamma_5 M^{-1}(x|x)) , \end{aligned} \quad (3)$$

which is a sum of fermionic connected and disconnected terms with traces to be taken in the spin and colour spaces. In the rest of the paper we shall refer to them as ‘one-loop’ and ‘two-loop’ contributions, respectively. The momentum zero projection

$$C_{\eta'}(t) \equiv \langle \eta'(t) \eta'(0) \rangle_{conn} - \langle \eta'(t) \eta'(0) \rangle_{disc} \quad (4)$$

is expected to decay exponentially,  $\sim \exp(-m_{\eta'} t)$  and reveal the flavour singlet mass,  $m_{\eta'}$ . On an antiperiodic (of length  $T$  in time) lattice one should encounter the usual cosh behaviour at large values of  $t$  and  $T - t$

$$G(t) \rightarrow \exp(-m_{\eta'} t) + \exp(-m_{\eta'} (T - t)) . \quad (5)$$

From this parametrization local effective masses  $m_{\eta'}(t)$  can be retrieved by solving the implicit equations

$$\frac{G(t+1)}{G(t)} = \frac{\exp(-m_{\eta'}(t+1)) + \exp(-m_{\eta'}(T-t-1))}{\exp(-m_{\eta'} t) + \exp(-m_{\eta'}(T-t))} , \quad (6)$$

where the *l.h.s.* ratios are taken from the lattice.

## 2.2 Diagonal improved stochastic estimator

Obviously the momentum zero projection embodied in eq. 3 requires the knowledge of the traces,  $\text{tr}(\gamma_5 M^{-1}(x|x))$ , on each time slice. But their exact evaluation is far beyond the scope of present computers.

One therefore takes resort to a stochastic estimate of the disconnected diagrams by introducing an ensemble of  $N_e$  nonlocal sources,  $\phi(x)^a$ ,  $a = 1, \dots, N_e$  with uncorrelated stochastic entries on the lattice sites  $x \in \text{colour} \times \text{spin} \times R_4$

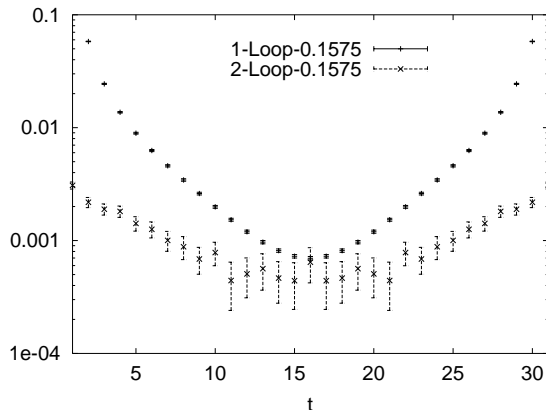


Figure 1: Correlation functions on the small lattice at the lightest sea quark mass,  $\kappa = 0.1575$ , with local sources. Upper (lower) curves refer to one-loop (two-loop) contributions.

space such that in the limit  $N_e \rightarrow \infty$  the ensemble averages show the following limiting behaviours

$$\langle \phi(x) \rangle \equiv \frac{1}{N_e} \sum_{a=1}^{N_e} \phi^a(x) \rightarrow 0 \quad (7)$$

$$\langle \phi(x)^\dagger \phi(y) \rangle \rightarrow \delta_{x,y} . \quad (8)$$

In our case, we chose  $Z_2$  noise for the components of the source vectors. By solving the Dirac equation

$$M(z, x)\xi(x) = \phi(z) \quad (9)$$

on the stochastic sources  $\phi(z)$  one retrieves a bias free estimate for the inverse Dirac operator in the large  $N_e$  limit

$$\langle \phi(y)^\dagger \xi(x) \rangle = \sum_z M^{-1}(z, x) \langle \phi(y)^\dagger \phi(z) \rangle \rightarrow M^{-1}(y, x) , \quad (10)$$

and hence for the one-loop term,  $\text{tr}(\gamma_5 M^{-1})$ . But beware of the subleading terms when computing components of  $M^{-1}$  as we do here (actually in spin space); for they might be affected by the dominant diagonal ones in so far the latter are not sufficiently rejected by our approximation to the Kronecker  $\delta$  in eq. 8. So we improve the estimate on nondiagonals,  $M^{-1}(y, x)$  ( $x \neq y$ ), by

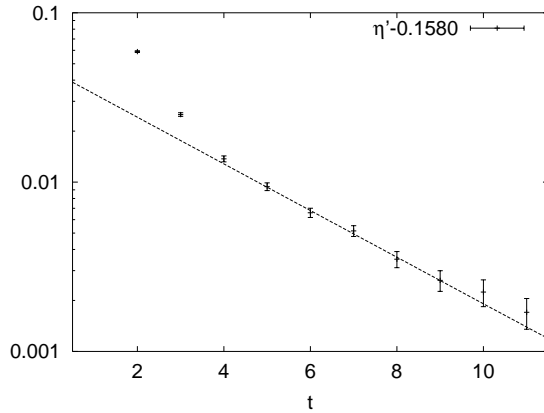


Figure 2:  $\eta'$  propagators ( $\kappa = 0.158$ ) with local source and sink on the large lattice.

subtracting out, from the expression on the *l.h.s.* of eq. 10, those leading error terms by redefining the estimator to be<sup>8</sup>:

$$\langle \phi(y)^\dagger \xi(x) \rangle - M^{-1}(x, x) \langle \phi(y)^\dagger \phi(x) \rangle = M^{-1}(y, x) + \sum_{z \neq x, y} M^{-1}(z, x) \langle \phi(y)^\dagger \phi(z) \rangle. \quad (11)$$

Note that in this improvement step, the subleading term on the *l.h.s.* again is gained by SET. Throughout this work we shall apply eq. 11 in order to achieve improved estimates to  $\text{tr}(\gamma_5 M^{-1})$ . We mention in passing that an alternative route would be to work in a spin explicit mode by using spin projected sources<sup>8,9</sup>.

### 2.3 Quality of the signal

In Table 1 we collected the characteristic parameters of our present analysis. We have used five different sea quark masses and two different lattice sizes to have some control on finite-size effects. While the number of vacuum configurations varies from 156 to 195, the number of independent stochastic sources has been chosen to be 400 (100) for the small (large) lattices. The pseudoscalar and vector mass ratios quoted refer to our final spectrum analysis<sup>10</sup>. The results presented in this talk are based on local sources only. The errors quoted are statistical and have been obtained by jackknifing.

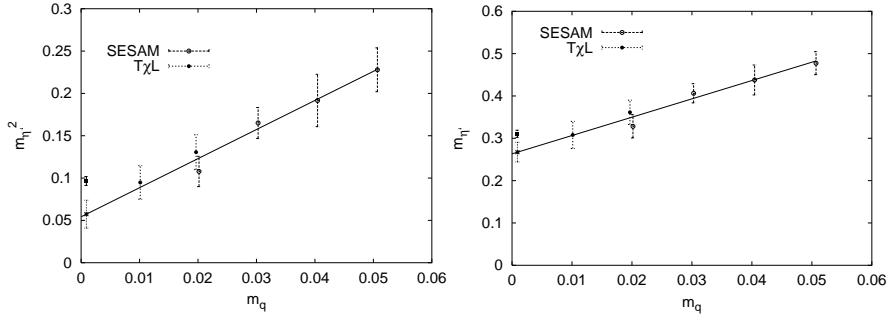


Figure 3: Chiral extrapolation of  $m_{\eta'}^2$  (left) and  $m_{\eta'}$  (right), both linear in the quark mass. Masses in lattice units. Full squares: pseudoexperimental value, according to eq. 16.

As a result we obtain two-loop correlators,  $C_{disc}(t)$ , with statistical quality illustrated for our lightest quark mass on the small lattice in Fig. 1. The plot also contains the connected correlator,  $C_8(t)$ , corresponding to the nonsinglet pseudoscalar meson, in order to demonstrate the reduced accuracy of the (Zweig-rule forbidden) two-loop contribution. At the time separation  $t \simeq 10$ , we are faced with a statistical error of order  $\approx 25\%$  on the latter.

Given this situation it is practically impossible to establish an effective mass plateau in the  $\eta'$  channel,  $C_{\eta'}(t)$ , (eq. 3). For further analysis we made single exponential fits to  $C_{\eta'}(t)$  and  $C_8(t)$  over the t-ranges listed in Table 1. The quality of our fits is illustrated for the lightest quark mass on the large lattice in Fig. 2.

### 3 Physics results

#### 3.1 Chiral extrapolations

Because of the well-known technical limitations of the hybrid Monte Carlo algorithm<sup>11</sup>, the SESAM and T $\chi$ L configurations correspond to two mass degenerate light sea quark flavours ( $N_f = 2$ ), with the unrenormalized mass value (in lattice units)

$$m_q = 1/2(\kappa^{-1} - \kappa_c^{-1}). \quad (12)$$

From our previous light spectrum analysis<sup>12</sup>, we quote the lattice spacing

$$a_\rho^{-1}(\kappa_l) = 2.302(64)\text{GeV} \quad (13)$$

and the critical and light quark  $\kappa$  values:

$$\kappa_c = .158507(44) \quad , \quad \kappa_{light} = .158462(42). \quad (14)$$

From our data we cannot decide whether it is  $m_{\eta'}^2$  or  $m_{\eta'}$  that follows a linear behaviour in the quark mass: the two fits shown in Fig. 3 work equally well, with  $\chi^2/d.o.f. \simeq \mathcal{O}(1)$ . Note that we make *no distinction* between sea and valence quarks, as we choose the quark masses in the fermion loops to equal the sea quark masses (symmetric extrapolation in the sense of ref. <sup>12</sup>).

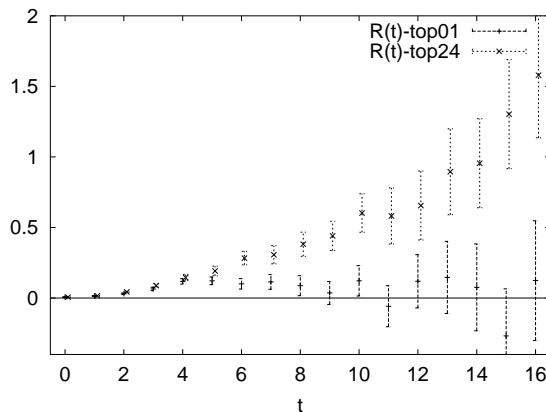


Figure 4: The sensitivity of the disconnected diagram,  $R_Q(t) := C_{disc}(t)/C_8(t)$ , when subsampling the vacuum configurations according to topological charge,  $|Q|$ .

In our  $N_f = 2$  world, according to eq. 3, we would not expect to encounter the full effect of Zweig rule forbidden diagrams, and hence we anticipate to underestimate the real world  $\eta'$  mass. From the experimental mass splitting

$$M_0^2 = M_{\eta'}^2 - M_8^2, \quad (15)$$

we therefore compute, in the spirit of the Witten-Veneziano formula eq. 1, the ‘pseudoexperimental’ value in the  $N_f = 2$  world:

$$M_{\eta'}^2(N_F = 2) = 2/3M_0^2 + M_\pi^2 = (716\text{MeV})^2. \quad (16)$$

This value corresponds in lattice units to the full squares in the two alternative chiral extrapolations shown in Fig. 3. To compare: our lattice analysis yields at the light quark mass

$$M_{\eta'}^2 = (551(85)\text{MeV})^2 \quad \text{and} \quad M_{\eta'} = 615(53)\text{MeV}, \quad (17)$$

by use of a linear ansatz in  $m_{\eta'}^2(m_q)$  and  $m_{\eta'}(m_q)$ , respectively.

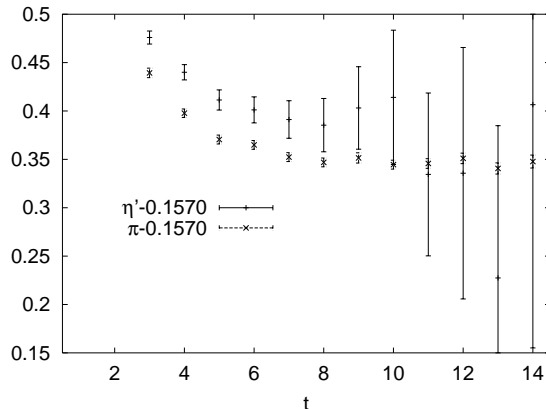


Figure 5: The effective local octet ( $\pi$ ) and singlet ( $\eta'$ ) masses after Wuppertal type smearing on source and sink.

### 3.2 Impact of topology

We expect two-loop diagrams to be sensitive to the topology of the vacuum. A simple check is to look for a dependency of the ratio of disconnected and connected correlators,  $R_Q(t)$ , on the size of the topological charge  $|Q|$ , as determined in ref.<sup>13</sup>. In Fig. 4, we have plotted, for  $\kappa_{sea} = .1575$  and the small lattice, the data with cuts according to  $|Q| \leq 1.5$  (top01) and  $|Q| > 1.5$  (top24). We definitely find a dependency of  $R_Q$  on  $|Q|$ . Note that the disconnected piece vanishes in the vacuum sector with small values of  $|Q|$ !

## 4 Discussion and outlook

The analysis presented here looks rather promising, but leaves room for further investigations:

**Smearing.** The  $\eta'$  correlator being a difference of one-loop and two-loop terms it is of great importance to *attain early asymptotics* of the flavour singlet correlator. But with local sources the connected (flavour octet) correlator does require analysis at  $t$ -values beyond 12, in view of appreciable excited state contributions. Yet for the flavour singlet situation, we had to analyse in the  $t$ -range 6 to 9, for lack of statistics. Thus it appears very promising to improve the ground state overlap by use of source and sink smearing; for this will help to establish mass plateaus in the flavour singlet channel and hence reduce errors. Indeed, we have observed mass plateaus appearing at  $t \simeq 4$  to 5, as illustrated

in Fig. 5. In a forthcoming paper, we shall elaborate on this point<sup>14</sup>.

**Spectral methods.** Another possible direction to go is to construct the two-loop correlator from the low lying eigenfunctions of the Dirac operator. For illustration we show in Fig. 6 the result of an attempt to saturate the spectral representation of the two-loop correlator by the 300 lowest eigenmodes of  $(\gamma_5 M)$ <sup>15</sup>. We find very nice agreement between the results from this eigenmode approach (EVA) from SET. This is very encouraging, since in the deeper chiral regime EVA will become even more efficient whereas the performance of SET will deteriorate.

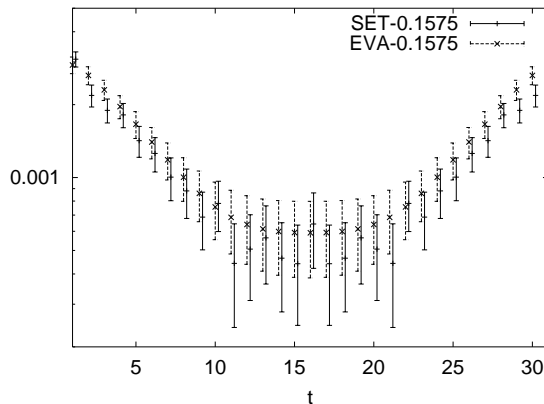


Figure 6: Saturation of the two-loop correlator with the 300 lowest eigenmodes of the operator  $(\gamma_5 M)$ , at the smallest sea quark mass on the small lattice. Symbols: crosses from EVA, horizontal lines from SET.

## Acknowledgements

T.S., H.N., and B.O. thank the DFG-Graduiertenkolleg “Feldtheoretische und Numerische Methoden in der Statistischen und Elementarteilchenphysik” for support. The HMC productions were run on an APE100 at NIC Zeuthen and INFN Roma while the loop computations were carried out on APE100 systems at DESY Zeuthen and at the University of Bielefeld. We are grateful to our colleagues F. Rapuano and G. Martinelli for the fruitful  $T\chi L$ -collaboration. Analysis was also performed on the CRAY T3E system of ZAM at Research Center Jülich. K.S. thanks the organizers of Confinement2000, in particular Prof. H. Suganuma, for inviting him to their very stimulating symposium.

## References

1. E. Witten, *Nucl. Phys. B* **156**, 269 (1979); G. Veneziano, *Nucl. Phys. B* **159**, 213 (1979).
2. G.S. Bali *et al* , *Phys. Lett. B* **309**, 378 (1993); J. Sexton *et al* , *Phys. Rev. Lett.* **75**, 4563 (1995); C.J. Morningstar *et al* , *Phys. Rev. D* **60**, 034509 (1999).
3. Y. Kuramashi *et al* , *Phys. Rev. Lett.* **72**, 3448 (1994).
4. G. Kilcup *et al* , *Nucl. Phys. Proc. Suppl. B* **47**, 358 (1996); L. Venkata-  
maran *et al* , *Nucl. Phys. Proc. Suppl. B* **53**, 259 (1997).
5. A. AliKhan *et al* , [CP-PACS - Collaboration], *Nucl. Phys. Proc. Suppl. B* **83-84**, 162 (2000).
6. Ch. Michael *et al* , [UKQCD - Collaboration], *Nucl. Phys. Proc. Suppl. B* **83-84**, 185 (2000).
7. Th. Lippert *et al* , [SESAM/T $\chi$ L - Collaboration], *Nucl. Phys. Proc. Suppl. A* **60**, 311 (1998).
8. J. Viehoff *et al* , [SESAM - Collaboration], *Nucl. Phys. Proc. Suppl. B* **63**, 269 (1998); *Nucl. Phys. Proc. Suppl. B* **73**, 856 (1999); J. Viehoff, DESY-THESIS-1999-036, WUB-DI-1999-17, Sep 1999, 94pp.
9. W. Wilcox in *Numerical Challenges in Lattice QCD*, eds. A. Frommer, Th. Lippert, B. Medeke, and K. Schilling, to appear in Lecture Notes in Computational Science and Engineering, (Springer, Heidelberg, 2000).
10. B. Orth *et al* , [SESAM - Collaboration], in preparation.
11. see e.g. the review of A.D. Kennedy, *Parallel Computing* **25** 1311 (1999).
12. N. Eicker *et al* , [SESAM - Collaboration], *Phys. Rev. D* **59**, 14509 (1999).
13. B. Alles *et al* , [SESAM - Collaboration], *Phys. Rev. D* **58**, 071503 (1998); Th. Lippert *et al* , [SESAM - Collaboration], *Nucl. Phys. Proc. Suppl. B* **73**, 521 (1999).
14. T. Struckmann *et al* , [SESAM - Collaboration], in preparation.
15. H. Neff *et al* , [SESAM - Collaboration], work in progress.